Biosensors and Bioelectronics 28 (2011) 204–209

Contents lists available at ScienceDirect

Biosensors and Bioelectronics

journal homepage: www.elsevier.com/locate/bios

Direct electrochemical reduction of graphene oxide on ionic liquid doped screen-printed electrode and its electrochemical biosensing application

Jianfeng Ping, Yixian Wang, Kai Fan, Jian Wu*, Yibin Ying

College of Biosystems Engineering and Food Science, Zhejiang University, Hangzhou 310058, PR China

ARTICLE INFO

Article history:
Received 28 March 2011
Received in revised form 29 June 2011
Accepted 11 July 2011
Available online 20 July 2011

Keywords:
Electrochemically reduced graphene oxide
Screen-printed electrode
Ionic liquid
NADH
Glucose

ABSTRACT

A novel electrochemical biosensing platform using electrochemically reduced graphene oxide (ER-GNO) modified electrode was proposed. This modified electrode was prepared by one-step electrodeposition of the exfoliated GNO sheets onto the ionic liquid doped screen-printed electrode (IL-SPE). The resulting ER-GNO/IL-SPE brought new capabilities for electrochemical devices by combining the advantages of ER-GNO and disposable electrode. Two important biomolecules, nicotinamide adenine dinucleotide (NADH) and hydrogen peroxide (H_2O_2), were employed to study the electrochemical performance of the ER-GNO/IL-SPE, which exhibited more favorable electron transfer kinetics than the bare IL-SPE. On the basis of the greatly enhanced electrochemical reactivity of H_2O_2 at the developed electrode, ER-GNO and glucose oxidase constructed disposable biosensor showed better analytical performance for the glucose detection compared with the IL-SPE based biosensor. The linear range for the detection of glucose was from 5.0 μM to 12.0 mM with a detection limit of 1.0 μM. This work provides a useful avenue for implementing ER-GNO as a new generation of electrochemical transducer in disposable electrode, which could expand the scope of graphene constructed electrochemical biosensing devices and hold great promise for routine sensing applications.

1. Introduction

Graphene, an up-rising star of carbon-based nanomaterial, is a sheet of sp^2 bonded carbon atoms that are arranged into a honeycomb structure, drawing tremendous attention from both the experimental and theoretical scientific communities since its discovery in 2004 (Novoselov et al., 2004). This unique nanostructure exhibits excellent electrical conductivity, mechanical strength, and chemical stability, which make it quite promising for the design of high sensitive and selective biosensors (Choi et al., 2010; Chowdhury et al., 2011; Pumera et al., 2010).

Like carbon nanotubes (CNTs), graphene provides a new and effective avenue for fabricating electrochemical biosensing devices in view of its large specific surface, good biocompatibility, and more importantly, its capability for promoting the electron transfer between electroactive species and electrodes (Garaj et al., 2010; Shao et al., 2010b; Yang et al., 2010). Graphene modified electrodes have been successfully applied to study or determine biomolecules, such as dopamine (Wang et al., 2009a), ascorbic acid (Keeley et al., 2010), glucose (Shan et al., 2009), nicotinamide adenine dinucleotide (NADH) (Zhou et al., 2009a), hydrogen peroxide (H_2O_2) (Lin et al., 2009), and DNA (Lim et al., 2010). Until now, the graphene films on the electrode surface are mostly prepared by drop-casting graphene dispersion solution obtained from chemically reduced graphene oxide (CR-GNO). However, such a preparation methodology always needs excessive toxic reducing agents (Chen et al., 2011; Stankovich et al., 2006), and moreover, some epoxides groups that cannot be fully removed by chemical treatment may degrade the electron mobility and further weaken the electrochemical performance (Guo et al., 2009; Shao et al., 2010a).

More recently, a novel strategy in graphene synthesis based on electrochemical method to produce electrochemically reduced graphene oxide (ER-GNO) has attracted considerable attention (Liu et al., 2008; Ramesha and Sampath, 2009; Zhou et al., 2009b). This method offers several advantages over other graphene fabrication techniques, including green, efficient, inexpensive, and rapid (Guo et al., 2009; Wang et al., 2009b). Moreover, by coupling with the spray-coating technique, the controllable synthesis of large-area and patterned ER-GNO films ranging from a single monolayer to several microns on various conductive substrates can be achieved (Zhou et al., 2009b). Despite such remarkable advantages of the synthesis as well as the excellent physicochemical properties of ER-GNO film, its electrochemical biosensing applications yet have not been explored so far.

Screen-printed electrodes (SPEs) have been widely used in electrochemical sensing due to the inherent superiority of their manufacturing process, which is inexpensive, rapid, simple and capable of mass production (Honeychurch and Hart, 2003; Kadara

* Corresponding author. Tel.: +86 571 88982180; fax: +86 571 88982180.
E-mail address: wujian69@zju.edu.cn (J. Wu).

0956-5663/$ – see front matter © 2011 Elsevier B.V. All rights reserved.
doi:10.1016/j.bios.2011.07.018

et al., 2009; Yang et al., 2008). Recently, our group reported an ionic liquid doped screen-printed electrode (IL-SPE) which exhibits high stability and electrochemical reactivity (Ping et al., 2010). In this work, a novel electrochemical biosensing device using ER-GNO film modified IL-SPE (ER-GNO/IL-SPE) was developed. The film was prepared by electrochemical deposition of the exfoliated GNO onto the surface of IL-SPE. A study concerning the electrodeposited process of ER-GNO film was carried out. Two kinds of common biomolecules, NADH and H_2O_2, were employed to investigate the electrochemical performance of the developed ER-GNO/IL-SPE. The electrooxidation of NADH has received extensive interest due to its important role as a cofactor in a whole diversity of dehydrogenase-based bioelectrochemical devices such as biosensors, biofuel cells, and bioreactors (Radoi and Compagnone, 2009). The determination of H_2O_2 is of great importance in virtue of the nature of H_2O_2 as a common intermediate in many biological reactions and an important parameter for the monitoring of these bioprocesses (Ping et al., 2011). A glucose sensor based on ER-GNO/IL-SPE and glucose oxidase (GOD) was further constructed and exhibited very attractive analytical performance for the glucose determination.

2. Experimental

2.1. Reagents

Reduced form of β-nicotinamide adenine dinucleotide (NADH), uric acid (UA), dopamine (DA), ascorbic acid (AA), hydrogen peroxide (H_2O_2, 30 wt%), glucose oxidase (GOD, E.C. 1.1.3.4, type II-S, from *Aspergillus niger*), and bovine serum albumin (BSA) were purchased from Sigma. Graphite powder (320 mesh, spectral pure), glucose, and *N*,*N*′-dimethylformamide (DMF) were obtained from Sinopham Chemical Reagent Co., Ltd. (Shanghai, China). Ionic liquid *n*-octylpyridinum hexafluorophosphate (OPPF) was purchased from Shanghai Chengjie Co., Ltd. (Shanghai, China). All other chemicals were of analytical grade and used without further purification. Except the note, sodium phosphate buffer solution (Na-PBS, 0.1 M, pH 7.0) was used as the electrolyte solution. Millipore-Q (18.2 MΩ cm) water was used for all experiments.

2.2. Preparation of GNO

Graphite oxide (GO) was synthesized from graphite powder by using a modified Hummers method (Hummers and Offeman, 1958; Kovtyukhova, 1999). Briefly, 2 g of graphite powder was added into a mixed solution of 20 mL of concentrated H_2SO_4, 1 g of $K_2S_2O_8$, and 1 g of P_2O_5, and the solution was kept at 80 °C for 4 h. Then, the mixture was carefully diluted with distilled water, and the resulting preoxidized product was filtered and dried. After this preoxidization process, the graphite was put into 50 mL of concentrated H_2SO_4. Then, 6 g of $KMnO_4$ was added gradually under stirring and ice-cooling to ensure that the temperature of the mixture was below 20 °C. The mixture was then stirred at 35 °C for 2 h, followed by adding 100 mL of distilled water. After 1 h, another 300 mL of distilled water was added to dilute the solution and then 5 mL of 30% H_2O_2 was injected into the solution to terminate the reaction. A bright yellow solution was obtained. The mixture was filtered and washed with HCl (3%) solution, and the obtained GO was suspended in distilled water.

Exfoliation of GO to graphene oxide (GNO) was achieved by ultrasonication of GO dispersion (0.5 wt%) using a supersonic cleaner (SK3300HP, 180 W, Shanghai, China). The obtained brown dispersion solution was then subjected to 20 min of centrifugation at 3000 r.p.m. to remove any unexfoliated GO. The resulted GNO (15 mg L^{-1}) was resuspended in sodium phosphate buffer solution (Na-PBS, 1.0 M, pH 4.12). The suspension of chemically reduced GNO (CR-GNO) in DMF was prepared according to the previous report (Park et al., 2009).

2.3. Preparation and modification of electrode

Ionic liquid *n*-octylpyridinum hexafluorophosphate doped screen-printed electrode (IL-SPE) was fabricated according to our previous work (Ping et al., 2010). The working area of the IL-SPE was calculated as 0.08 cm^2 (4 mm × 2 mm) with an 8 mm × 2 mm connecting strip. Prior to the modification, the electrode surface was washed with distilled water and dried in nitrogen atmosphere. Electrochemical reduction of GNO on the IL-SPE surface was performed in the nitrogen purged GNO dispersion solution (0.5 mg L^{-1}) with a magnetic stirrer at a working potential of −0.8 V (vs. Ag/AgCl) applied for 600 s. For comparison, the CR-GNO film modified IL-SPE (CR-GNO/IL-SPE) was prepared by drop-casting 20 μL of CR-GNO-DMF suspension on the IL-SPE surface and dried at room temperature in the air for 2 h, while the GNO sheets modified IL-SPE (GNO/IL-SPE) was prepared by drop-casting 20 μL of GNO dispersion on the IL-SPE.

For fabricating GOD-based bioelectrodes, a 1 wt% aqueous solution of BSA was mixed with GOD at the volume ratio of 1:2 to give a GOD-BSA mixture, and 6 μL of the resulting mixture was coated onto the ER-GNO/IL-SPE and IL-SPE. A 2 μL aqueous solution of glutaraldehyde (40 mM) was further coated onto electrodes to cross-link the GOD onto the electrode. The as-prepared electrodes were rinsed with distilled water and dried in air. After these processes, the GOD/ER-GNO/IL-SPE and GOD/IL-SPE were transferred into Na-PBS (0.1 M, pH 7.0) for 15 min before use and stored in the same solution at 4 °C when are not used.

2.4. Instruments

All the electrochemical measurements were carried out on a CHI 440 electrochemical workstation (CH Instruments, USA). The electrochemical cell was assembled with a conventional three-electrode system: a saturated Ag/AgCl reference electrode, a Pt wire auxiliary electrode, and the prepared working electrode. Amperometric studies were carried out under stirred conditions. The sample solutions were purged with nitrogen for at least 30 min to remove oxygen prior to starting a series of experiments. The scanning electron microscopy (SEM) experiment was made on a Philips XL-30 ESEM. All the experiments were performed at 25 ± 1 °C.

3. Results and discussion

3.1. Electrochemical reduction of GNO

Fig. 1A shows the typical linear sweep voltammograms of the IL-SPE in the absence and presence of GNO at the potential range from 0 to −1.2 V. In the absence of GNO, the IL-SPE revealed no peaks (Fig. 1A(a)). On the addition of GNO, the cathodic current started to increase at −0.58 V and reached at the maximum at −0.70 V (Fig. 1A(b)). This large peak should be attributed to the reduction of some functional groups on the exfoliated GNO sheets. To investigate which groups were reduced during the potential sweep, the linear sweep response of the CR-GNO film modified IL-SPE (CR-GNO/IL-SPE) in the blank buffer solution was also recorded. As shown, no reduction peak was found (Fig. 1A(c)). Given a large amount of oxygen functional groups on the GNO, such as –OH, –COOH, and epoxides, compared with those on chemically reduced CR-GNO (Wang et al., 2009b), the reduction peak at the IL-SPE obtained in the GNO dispersion solution could be due to the reduction of the surface oxygen groups (Guo et al., 2009). These results

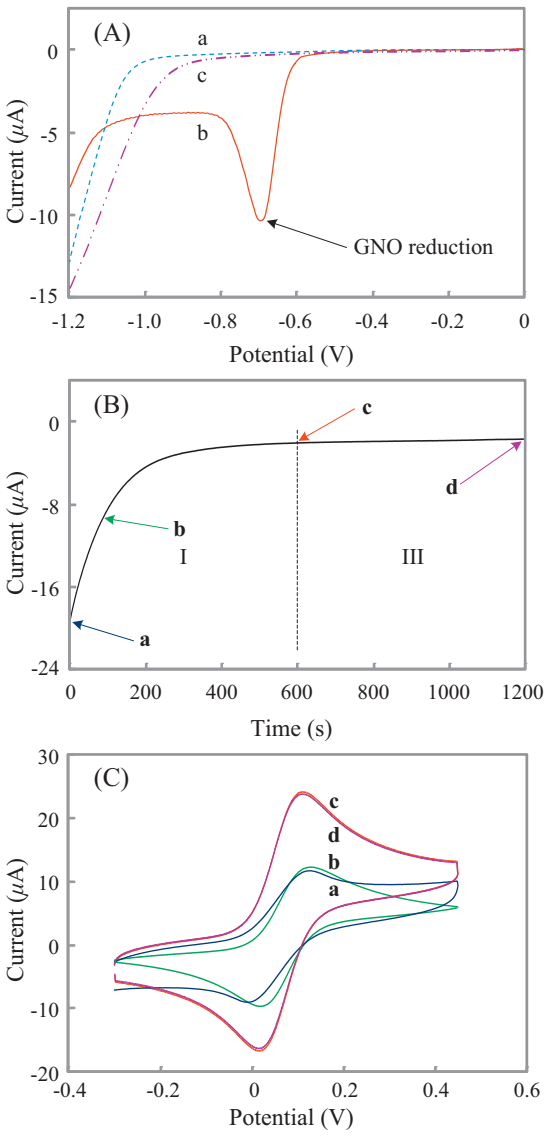

Fig. 1. (A) Linear sweep voltammograms of the IL-SPE in the absence (a) and presence (b) of GNO, curve (c) recorded at the CR-GNO/IL-SPE in the absence of GNO, electrolyte: nitrogen purged Na-PBS (1.0 M, pH 4.12); (B) typical *i–t* curve for electrochemical reduction of GNO at the IL-SPE in Na-PBS (1.0 M, pH 4.12) at −0.8 V (vs. Ag/AgCl); (C) cyclic voltammograms for 1.0 mM $[Fe(CN)_6]^{3-/4-}$ in 0.1 M KCl obtained at different phases on the deposited curve in B. Scan rate: 50 mV s^{-1}.

demonstrated that the exfoliated GNO could be reduced electrochemically onto the electrode surface.

Potentiostatic method was employed for the one-step electrodeposition of the exfoliated GNO onto the IL-SPE surface to produce ER-GNO film. As shown in Fig. 1B, with the extension of the electrochemical reduction time, the current decreased slowly during the period of the first 600 s, then reached the background level gradually. At the same time, an obvious change in color from yellow-brown to black at the electrode surface was observed, indicating the restoration of the π network with the carbon structure, which has been witnessed during the synthesis of CR-GNO (Li et al., 2008). This deposition process was similar to that reported by Zhou et al., in which they used a model involved conductor/insulator/electrolyte three-phase interlines to explain the electrolysis of GNO films on various substrates (Zhou et al., 2009b).

To further study the electrodepositing process of ER-GNO film on the IL-SPE surface, the redox couple $[Fe(CN)_6]^{3-/4-}$ was employed. Fig. 1C displays the cyclic voltammograms about ER-GNO deposited IL-SPE at the different phases on the *i–t* deposition curve. At the bare IL-SPE (namely the phase a on *i–t* curve), well-defined peak with a small peak potential separation of 110 mV was observed (Fig. 1C(a)). With the electrochemical reduction of GNO (namely the phase b on the *i–t* curve), the surface conductivity was gradually enhanced and hence the reversibility of $[Fe(CN)_6]^{3-/4-}$ was improved (Fig. 1C(b)). After the electrode surface turning to black (namely the phase c on the *i–t* curve), the electrode exhibited higher cyclic response with the smaller peak separation of 80 mV (Fig. 1C(c)). No improvement of the response was observed with further electrolysis (Fig. 1C(d), namely the phase d on the *i–t* curve), suggesting the complete cover of ER-GNO on the electrode surface. The SEM image of the prepared ER-GNO film was shown in Fig. 2, which presents uniform surface topography.

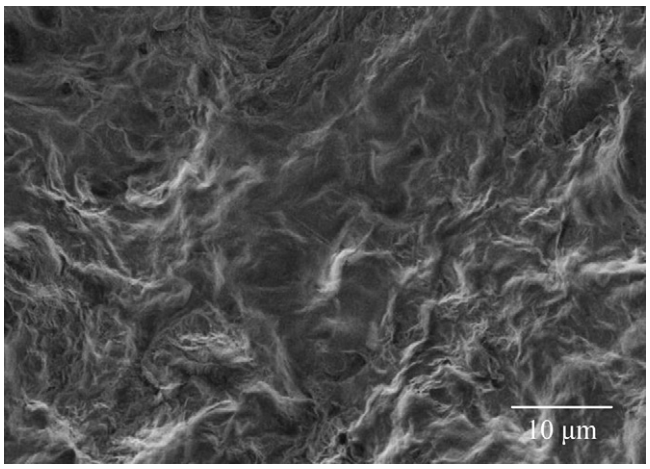

Fig. 2. SEM image of the ER-GNO/IL-SPE surface.

3.2. Electrochemical response of ER-GNO/IL-SPE to NADH

Fig. 3 shows the cyclic voltammograms of the bare and modified electrodes in Na-PBS (0.1 M, pH 7.0) without and with 1.0 mM NADH. The oxidation of NADH at the bare IL-SPE occurred at the potential of +0.60 V (Fig. 3A). While at the ER-GNO/IL-SPE, it exhibited a substantial negative shift of the oxidation peak potential to +0.38 V (Fig. 3D), indicating the presence of ER-GNO film made the electron transfer easier. Moreover, the peak current at the ER-GNO/IL-SPE was twice larger than that of the IL-SPE. The NADH oxidation at the GNO/IL-SPE exhibited poor peak current with peak potential of +0.72 V (Fig. 3B), suggesting the sluggish electron transfer at the interface due to the poor conductivity of GNO (Chen et al., 2011). In the case of ER-GNO, the high density of edge-plane-like defective sites on ER-GNO film may offer some favorable sites for transferring the electron to biomolecules and would facilitate/accelerate the electron transfer between electrode surface and electroactive species in solution (Guo et al., 2009; Zhou et al., 2009b). The response of the ER-GNO/IL-SPE for the NADH oxidation was also superior to that of CR-GNO/IL-SPE (+0.44 V, Fig. 3C). Since the toxic reducing agents are always involved during the synthesis of CR-GNO (Stankovich et al., 2006; Zhou et al., 2009a), the ER-GNO approach should be more suitable for the electrode preparation. The peak potential of NADH oxidation at the ER-GNO/IL-SPE was lower than those at gold nanomaterials modified electrodes (+0.52 V (Qiu et al., 2009) or +0.53 V (Shan et al., 2008)), and was comparable with those at CNTs modified electrodes (+0.40 V (Zhang et al., 2004) or +0.36 V (Musameh et al., 2002)), nevertheless our electrodes are inexpensive and easy to be prepared.

Another attractive feature of the ER-GNO/IL-SPE was its highly stable amperometric response and antifouling properties towards

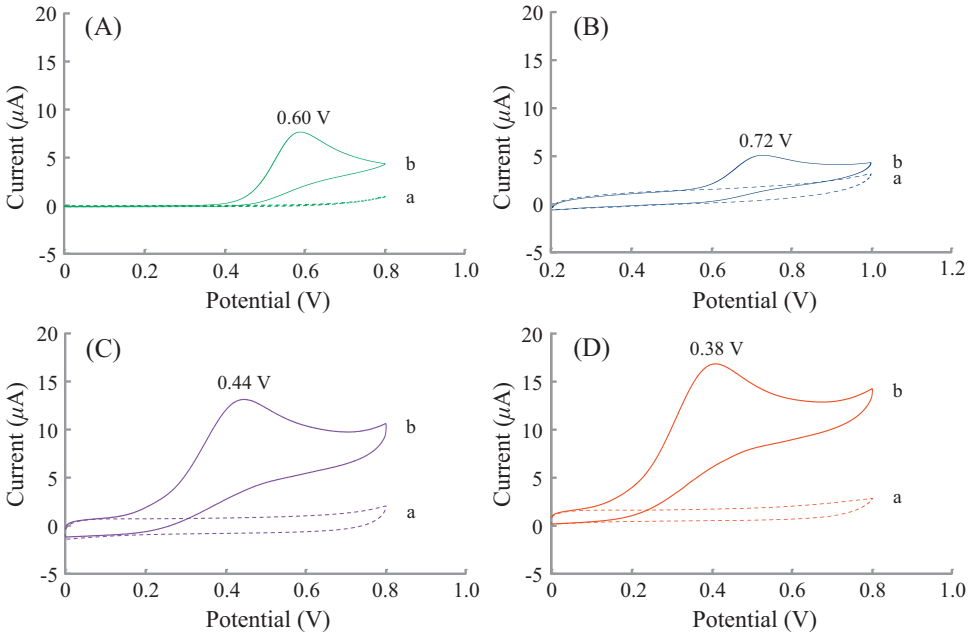

Fig. 3. Cyclic voltammograms of the IL-SPE (A), GNO/IL-SPE (B), CR-GNO/IL-SPE (C) and ER-GNO/IL-SPE (D) in Na-PBS (0.1 M, pH 7.0) in the absence (a) and presence (b) of 1.0 mM NADH. Scan rate: 50 mV s^{-1}.

the oxidation of NADH. Fig. 4A compares the amperometric response to 1.0 mM NADH, as recorded over a continuous 60 min period, at the bare GCE and ER-GNO/IL-SPE held at +0.6 V. As shown, the bare GCE exhibited a rapid decay of the current (up to 55%) after 60 min, which indicated the poor surface antifouling ability. On the contrary, the response of the ER-GNO/IL-SPE remained quite stable throughout the entire period, with only 2%, 4%, and 10% current diminutions at 10 min, 30 min, and 60 min, respectively. This good stability of the ER-GNO/IL-SPE is comparable with those of carbon nanotubes (Kachoosangi et al., 2009) or ionic liquid (Maleki et al., 2006) modified electrodes. Compton et al. reported that the high density of edge-plane-like defective sites on carbon materials may induce the resistance to fouling (Banks and Compton, 2005). This means the more edge-plane-like defective sites on ER-GNO compared with those on GCE may play an important role in minimizing passivation effects for NADH oxidation.

In the determination of NADH, the interference from ascorbic acid (AA) is a major problem due to the fact that these two biomolecules are oxidized at almost the same potential at the traditional electrodes, resulting in the overlap of voltammetric response (Radoi and Compagnone, 2009). Fig. 4B shows the cyclic voltammogram of equal concentrations of AA and NADH in 0.1 M PBS (pH 7.0) obtained at the ER-GNO/IL-SPE. Two well-defined and resolved voltammetric peaks were observed for the electrochemical oxidation of AA and NADH, respectively. It should be noted that the peak separation for the oxidation of AA and NADH was 220 mV, which is large enough to resolve the voltammetric peaks. These demonstrate that the ER-GNO/IL-SPE could be used to detect NADH in the presence of AA without interference.

The high electrocatalytic activity, low susceptibility to electrode fouling, and insensitivity to interference from AA make the ER-GNO/IL-SPE very attractive for the amperometric measurement of NADH. As shown in Fig. S1 (Supporting Information), the current increased with the addition of NADH, indicating the stable and efficient electrocatalytic activity of the ER-GNO/IL-SPE. Moreover, the oxidation current of NADH displayed good linearity with the concentration range from 10 μM to 2.0 mM. The detection limit was evaluated as 2.0 μM (S/N = 3). Repetitive measurements of 50.0 μM

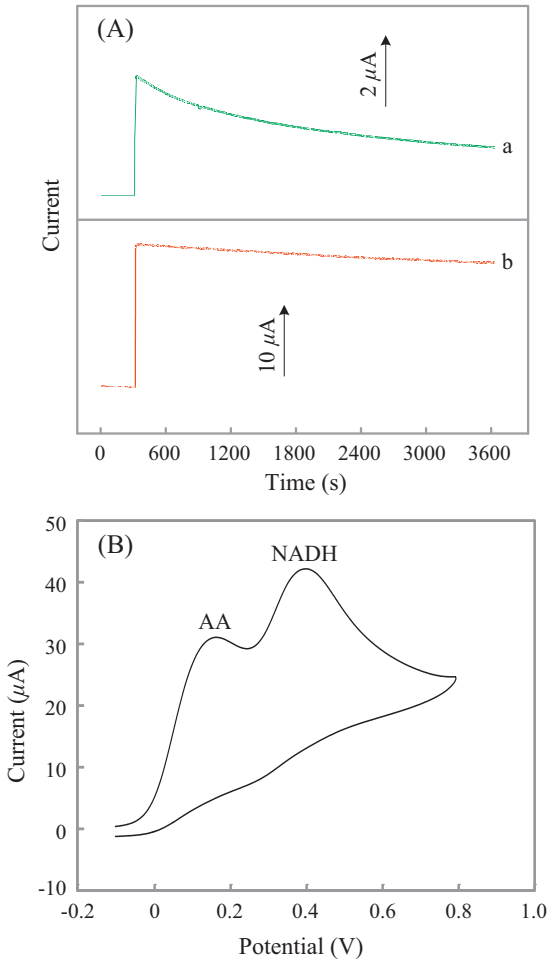

Fig. 4. (A) The response stability of the bare GCE (a) and ER-GNO/IL-SPE (b) to 1.0 mM NADH in Na-PBS (0.1 M, pH 7.0) at +0.6 V (vs. Ag/AgCl); (B) cyclic voltammogram of the ER-GNO/IL-SPE in Na-PBS (0.1 M, pH 7.0) containing 2.0 mM AA and 2.0 mM NADH. Scan rate: 50 mV s^{-1}.

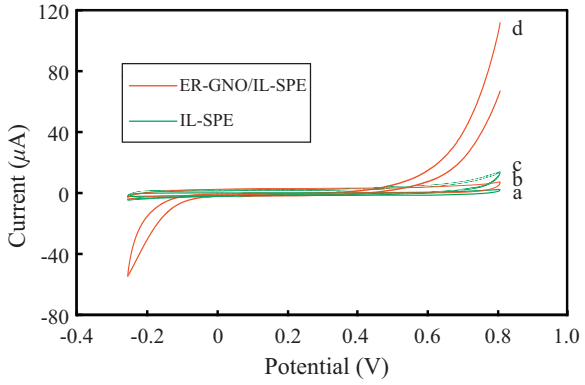

Fig. 5. Cyclic voltammograms of the IL-SPE (a and c) and ER-GNO/IL-SPE (b and d) in Na-PBS (0.1 M, pH 7.0) in the absence (a and b) and presence (c and d) of 4.0 mM H_2O_2. Scan rate: 50 mV s^{-1}.

NADH showed good reproducibility with a relative standard deviation (RSD) of 3.8% (n = 10), while RSD was 4.5% for six electrodes.

3.3. Electrochemical response of ER-GNO/IL-SPE to H_2O_2

Fig. 5 shows the cyclic voltammograms of the bare IL-SPE and ER-GNO/IL-SPE in the absence and presence of 4.0 mM H_2O_2. It is clear that the oxidation and reduction of H_2O_2 at the ER-GNO/IL-SPE commenced at +0.45 V and 0 V, respectively (Fig. 5(d)). On the contrary, there was no obvious reduction current for H_2O_2 at the IL-SPE over most of the potential range, and only small oxidation current was observed which occurred at much higher potential of +0.75 V (Fig. 5(c)). Such a superior electrocatalytic activity of ER-GNO/IL-SPE towards H_2O_2 could be ascribed to the fast electron transfer rate at the interface, probably owing to the high density of edge-plane-like defective sites on ER-GNO (Guo et al., 2009; Zhou et al., 2009b). The improved response and lower potential towards H_2O_2 may enable the ER-GNO/IL-SPE to be a promising candidate for fabricating oxidase-based amperometric biosensors by utilizing this unique ER-GNO material.

Fig. 6 compares the amperometric response (at +0.5 V (A) and at −0.2 V (B)) of the IL-SPE (a) and ER-GNO/IL-SPE (b) to successive additions of 0.1 mM H_2O_2. As expected from the voltammetric data, the IL-SPE hardly responded to these concentration changes under these low detection potentials. The ER-GNO/IL-SPE, however, exhibited rapid response towards the increase of H_2O_2 level in solution, producing steady-state signals within 4 ± 1 s. Moreover, the oxidation and reduction current of H_2O_2 displayed good linearity in the concentration range from 0.1 μM to 2.0 mM and from 0.15 μM to 1.8 mM, respectively. The linear equation was calibrated as I_{ox} (μA) = −0.035 + 6.286 C (mM) with a correlation coefficient of 0.9990 for the oxidation of H_2O_2, while for the reduction of H_2O_2, it was calculated as I_{re} (μA) = −0.086 + 4.278 C (mM) with a correlation coefficient of 0.9992. The detection limits for the oxidation and reduction of H_2O_2 were calculated as 0.05 μM and 0.08 μM, respectively (S/N = 3).

Additionally, the selectivity of ER-GNO/IL-SPE towards H_2O_2 reduction in the presence of several potential interferences, such as ascorbic acid (AA), uric acid (UA) and dopamine (DA), was evaluated. As shown in Fig. S2 (Supporting Information), an obvious current response was observed with the addition of 0.01 mM H_2O_2, whereas the response current was kept almost at the same value after the additions of various interferences. The response current of the final addition of H_2O_2 was the same as that of first addition, suggesting that those interferences did not affect the reduction of H_2O_2 at the ER-GNO/IL-SPE. These results suggested that the ER-GNO film modified IL-SPE can be used to selectively detect H_2O_2 in the presence of potential interferences, which may provide a favorable electrochemical biosensing platform for routing sensing and practical applications.

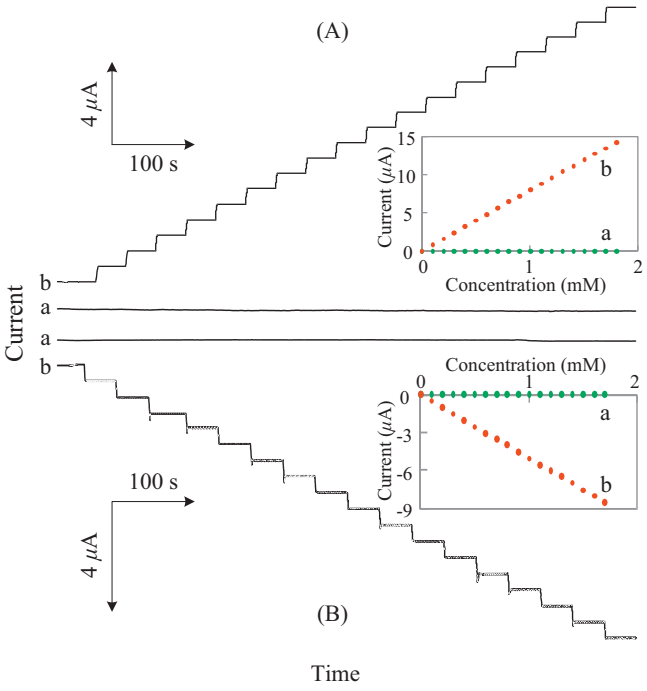

Fig. 6. Current–time curves of the IL-SPE (a) and ER-GNO/IL-SPE (b) with successive additions of 0.1 mM H_2O_2 measured at +0.5 V (A) and −0.2 V (B). *Inset*: Calibration curves for H_2O_2 at the IL-SPE (a) and ER-GNO/IL-SPE (b). Electrolyte: 0.1 M Na-PBS (pH 7.0).

3.4. Amperometric biosensing of glucose

The greatly enhanced electrochemical reactivity of H_2O_2 at the ER-GNO/IL-SPE could be further exploited to design oxidase-based amperometric biosensors. As an example, the glucose biosensor based on GOD and ER-GNO was constructed. Fig. S3 (Supporting Information) displays the steady-state response at different electrodes with the applied potential of −0.2 V on the injection of various concentration of glucose into Na-PBS (0.1 M, pH 7.0). As shown, the GOD/IL-SPE did not respond to the addition of glucose under this low applied potential. Nevertheless, in the case of ER-GNO based bioelectrode, it offered substantially larger signals reflecting the excellent electrocatalytic activity of GOD/ER-GNO/IL-SPE. The current increased linearly with glucose concentration over the range from 5.0 μM to 10.0 mM with the sensitivity of 22.78 μA mM^{-1} cm^{-2}. The detection limit was estimated to be 1.0 μM (S/N = 3). The comparison of the analytical performance of glucose determination at the developed electrode with other electrodes reported previously was summarized in Table S1 (Supporting Information). It can be seen that the GOD/ER-GNO/IL-SPE exhibited wider linear range, lower detection limit and higher sensitivity for the determination of glucose.

To evaluate the selectivity of the GOD/ER-GNO/IL-SPE, the common interfering biomolecules, AA, UA and DA, which normally coexist with glucose in real samples, were examined. As expected, these three biomolecules (concentration 0.2 mM) resulted in negligible signals at the applied potential of −0.2 V, while an obvious response was found with the addition of 0.1 mM glucose (data not shown). The reproducibility of the single bioelectrode was investigated by repetitive detection of 0.1 mM glucose. The RSD was 3.04% for 30 successive assays. On the other hand, the reproducibility of electrode-to-electrode was checked by the measurement of 0.1 mM glucose. Five GOD/ER-GNO/IL-SPEs prepared under the same con-

ditions were tested and the RSD was found to be 3.52%, confirming that the fabrication method was highly reproducible.

The bioelectrodes were also investigated for their operational and storage stability. The operational stability of the sensor was evaluated by observing the change of response current of 0.1 mM glucose in the stirred Na-PBS (0.1 M, pH 7.0). During the measurement, the current response did not decrease in the first 20 min, whereas the current at 50 and 100 min were 96% and 91% of the initial value, respectively. Meanwhile, the storage stability of the proposed electrode was investigated over a week. Its sensitivity towards glucose was checked every day. After stored at 4 °C for a week, the response current of 0.1 mM glucose at the GOD/ER-GNO/IL-SPE remained 93.7% of the initial value.

To illustrate the feasibility of the developed GOD/ER-GNO/IL-SPE for routine analysis, the electrode was applied to determine glucose concentration in the milk sample. The sample was diluted with Na-PBS (0.1 M, pH 7.0) at a volume ratio of 1:9. The analytical results were summarized in Table S2 (Supporting Information). One can see that the proposed bioelectrode exhibited exact recovery results, indicating the potential application of GOD/ER-GNO/IL-SPE for determination of glucose in real sample.

4. Conclusions

In this work, a novel and disposable electrochemical biosensing device based on ER-GNO film modified screen-printed electrode was proposed. The 'green' ER-GNO film was prepared by one-step electrodeposition of the exfoliated GNO sheets onto the surface of IL-SPE. The $[Fe(CN)_6]^{3-/4-}$ redox probe was employed to characterize the electrodepositing process of ER-GNO. With the high density of edge-plane-like defective sites on ER-GNO, the developed ER-GNO/IL-SPE possessed very excellent electrocatalytic activity towards biomolecules NADH and H_2O_2. The substantial decrease in the overpotential of H_2O_2 reduction at the ER-GNO/IL-SPE promotes the GOD and ER-GNO constructed bioelectrode to be an effective low-potential amperometric biosensor for glucose sensing. This work reveals that ER-GNO could be a favorable and promising carbon electrode material for constructing other electrochemical oxidase-based biosensors, which may have wide potential applications in biocatalysis, bioelectronics and biofuel cells.

Acknowledgement

We are grateful for the financial supports from the Key Scientific Project of China (No. 2009ZX08012-004B).

Appendix A. Supplementary data

Supplementary data associated with this article can be found, in the online version, at doi:10.1016/j.bios.2011.07.018.

References

Banks, C.E., Compton, R.G., 2005. Analyst 130, 1232–1239.
Chen, L.Y., Tang, Y.H., Wang, K., Liu, C.B., Luo, S.L., 2011. Electrochem. Commun. 13, 133–137.
Choi, B.G., Park, H., Park, T.J., Yang, M.H., Kim, J.S., Jang, S.Y., Heo, N.S., Lee, S.Y., Kong, J., Hong, W.H., 2010. ACS Nano 4, 2910–2918.
Chowdhury, R., Adhikari, S., Rees, P., Wilks, S.P., 2011. Phys. Rev. B 83, 045401.
Garaj, S., Hubbard, W., Reina, A., Kong, J., Branton, D., Golovchenko, J.A., 2010. Nature 467, 190–194.
Guo, H.L., Wang, X.F., Qian, Q.Y., Wang, F.B., Xia, X.H., 2009. ACS Nano 3, 2653–2659.
Honeychurch, K.C., Hart, J.P., 2003. Trac-Trends Anal. Chem. 22, 456–469.
Hummers, W.S., Offeman, R.E., 1958. J. Am. Chem. Soc. 80, 1339.
Kachoosangi, R.T., Musameh, M.M., Abu-Yousef, I., Yousef, J.M., Kanan, S.M., Xiao, L., Davies, S.G., Russell, A., Compton, R.G., 2009. Anal. Chem. 81, 435–442.
Kadara, R.O., Jenkinson, N., Banks, C.E., 2009. Sens. Actuators B 138, 556–562.
Keeley, G.P., O'Neill, A., McEvoy, N., Peltekis, N., Coleman, J.N., Duesberg, G.S., 2010. J. Mater. Chem. 20, 7864–7869.
Kovtyukhova, N.I., 1999. Chem. Mater. 11, 771–778.
Li, D., Müller, M.B., Gilje, S., Kaner, R.B., Wallace, G.G., 2008. Nat. Nanotechnol. 3, 101–105.
Lim, C.X., Hoh, H.Y., Ang, P.K., Loh, K.P., 2010. Anal. Chem. 82, 7387–7393.
Lin, W., Liao, C., Jhang, J., Tsai, Y., 2009. Electrochem. Commun. 11, 2153–2156.
Liu, N., Luo, F., Wu, H.X., Liu, Y.H., Zhang, C., Chen, J., 2008. Adv. Funct. Mater. 18, 1518–1525.
Maleki, N., Safavi, A., Tajabadi, F., 2006. Anal. Chem. 78, 3820–3826.
Musameh, M., Wang, J., Merkoci, A., Lin, Y.H., 2002. Electrochem. Commun. 4, 743–746.
Novoselov, K.S., Geim, A.K., Morozov, S.V., Jiang, D., Zhang, Y., Dubonos, S.V., Grigorieva, I.V., Firsov, A.A., 2004. Science 306, 666–669.
Park, S., An, J., Jung, I., Piner, R.D., An, S.J., Li, X., Velamakanni, A., Ruoff, R.S., 2009. Nano Lett. 9, 1593–1597.
Ping, J.F., Wu, J., Ying, Y.B., 2010. Electrochem. Commun. 12, 1738–1741.
Ping, J.F., Wu, J., Fan, K., Ying, Y.B., 2011. Food Chem. 126, 2005–2009.
Pumera, M., Ambrosi, A., Bonanni, A., Chng, E.L.K., Poh, H.L., 2010. Trac-Trends Anal. Chem. 29, 954–965.
Qiu, H.J., Xue, L.Y., Ji, G.L., Zhou, G.P., Huang, X.R., Qu, Y.B., Gao, P.J., 2009. Biosens. Bioelectron. 24, 3014–3018.
Radoi, A., Compagnone, D., 2009. Bioelectrochemistry 76, 126–134.
Ramesha, G.K., Sampath, S., 2009. J. Phys. Chem. C 113, 7985–7989.
Shan, C.S., Li, F.H., Yuan, F.Y., Yang, G.F., Niu, L., Zhang, Q., 2008. Nanotechnology 19, 285601–285606.
Shan, C.S., Yang, H.F., Song, J.F., Han, D.X., Ivaska, A., Niu, L., 2009. Anal. Chem. 81, 2378–2382.
Shao, Y.Y., Wang, J., Engelhard, M., Wang, C.M., Lin, Y.H., 2010a. J. Mater. Chem. 20, 743–748.
Shao, Y.Y., Wang, J., Wu, H., Liu, J., Aksay, I.A., Lin, Y.H., 2010b. Electroanalysis 22, 1027–1036.
Stankovich, S., Dikin, D.A., Geoffrey Dommett, H.B., Kohlhaas, K.M., Zimney, E.J., Stach, E.A., Piner, R.D., Nguyen, S.T., Ruoff, R.S., 2006. Nature 442, 282–286.
Wang, Y., Li, Y.M., Tang, L.H., Lu, J., Li, J.H., 2009a. Electrochem. Commun. 11, 889–892.
Wang, Z.J., Zhou, X.Z., Zhang, J., Boey, F., Zhang, H., 2009b. J. Phys. Chem. C 113, 14071–14075.
Yang, T.H., Hung, C.L., Ke, J.H., Zen, J.M., 2008. Electrochem. Commun. 10, 1094–1097.
Yang, W.R., Ratinac, K.R., Ringer, S.P., Thordarson, P., Gooding, J.J., Braet, F., 2010. Angew. Chem. Int. Ed. 49, 2114–2138.
Zhang, M.G., Smith, A., Gorski, W., 2004. Anal. Chem. 76, 5045–5050.
Zhou, M., Zhai, Y.M., Dong, S.J., 2009a. Anal. Chem. 81, 5603–5613.
Zhou, M., Wang, Y.L., Zhai, Y.M., Zhai, J.F., Ren, W., Wang, F.A., Dong, S.J., 2009b. Chem. Eur. J. 15, 6116–6120.